J Korean Radiol Soc 2008 ; 59 : 385-393

A Comparison between Dual-Exposure Dual-Energy Radiography and Standard Chest Radiography for the Diagnosis of Small Pulmonary Nodules[1]

Hye Sun Hwang, M.D., Myung Jin Chung, M.D., Sung Mok Kim, M.D., Jiwon Lee, M.D.[2], Heon Han, M.D.[2]

Purpose: To evaluate the utility of dual-exposure dual-energy radiography against the standard chest radiography in the discrimination of lung nodules and the presence of nodule calcification.

Materials and Methods: Twenty-nine patients with a total of 43 peripheral lung nodules were examined by dual-exposure dual-energy radiography (DER) and confirmed by a chest CT were included in the study. Of the identified peripheral lung nodules, 24 showed calcification and 19 did not. Further, 28 lesion-free regions from the same patient population were selected as negative controls. Two radiologists evaluated 71 marked locations using both standard chest radiographs (SR) and DER to determine whether the marked locations represented a true nodule, and whether nodule calcification was present. A continuous rating scale of 0–10 was used to represent each observer's confidence level. We calculated the areas under ROC curves (AUC) for SR alone and for DER, and performed a statistical analysis to compare the results.

Results: The ability to discriminate nodules was higher for DER than for SR. However, the was not statistically significant ($p = 0.202$). Inter-observer agreement was moderate regardless of if DER was used. The predictability of nodule calcification was significantly higher for DER compared to SR ($p < .001$). Moreover, inter-observer agreement was slight with SR alone but moderate with DER.

Conclusion: DER, in conjunction with SR, has no additional benefit in small lung nodule discrimination but does provide a significant benefit in the characterization of nodule calcification.

Index words : Lung diseases
Radiography, dual-energy scanned projection

[1]Department of Radiology and Center for Imaging Science, Samsung Medical Center, Sungkyunkwan University School of Medicine, Korea
[2]Department of Radiology, Kangwon National University College of Medicine, Korea
This article was presented at the 2006 RSNA scientific assembly.
This work was supported by the Korea Research Foundation Grant funded by the Korean Government (MOEHRD) (KRF-2005-041-D00956).
Received August 12, 2008 ; Accepted October 14, 2008
Address reprint requests to : Myung Jin Chung, M.D., Department of Radiology and Center for Imaging Science, Samsung Medical Center, Sungkyunkwan University School of Medicine, 50, Ilwon-dong, Kangnam-gu, Seoul 135-710, Korea
Tel. 82-2-3410-2519 Fax. 82-2-3410-2559 E-mail: mj1.chung@samsung.com

Despite the advances in diagnostic radiology, the chest radiography still represents the most common radiological modality since it is relatively low in cost and has a low radiation exposure. However, false negative diagnoses of pulmonary nodules have been reported to be as high as 18–32% (1–3). In part, this may be due to the obscuration by overlying bone and soft-tissue structures (4). The most reliable factor in determining the benignancy of a nodule by chest radiography is by nodule calcification (5). Thus, detecting pulmonary nodules and nodule calcification via a chest radiograph is important for chest radiologists.

This obscuration of diagnosis by bone and soft tissue may be corrected by selective images using dual-energy subtraction. For example, non-calcified lung nodules obscured by ribs can be identified on soft tissue selective images, whereas calcified nodules can be identified by bone-selective images.

Recently, full-field digital amorphous silicon flat-panel X-ray detector radiography systems based on cesium iodide (CsI) and amorphous silicon have become commercially available. These flat panel detectors show reduced noise and the potential for improved image quality (6–8).

The aim of our study was to evaluate the additional value provided by dual-exposure dual-energy radiography using a CsI flat-panel detector for the detection and discrimination of small lung nodules, and for the prediction of calcification in the nodule compared to the standard chest radiography alone.

Materials and Methods

Patients

Our institutional review board approved this retrospective study and waived the requirement for informed consent. Twenty-nine patients were randomly selected from the patients who visited our hospital to evaluate a solitary pulmonary nodule or nodule-mimicking lesion. Moreover, each patient underwent a routine clinical program, which included a dual-exposure dual-energy chest radiography and chest CT. Patients with other confounding diseases and opacities (such as pulmonary fibrosis and consolidation) were excluded from the study. The mean patient age was 54 years old (range 45–67).

Chest radiography and CT scanning

Chest radiographs were acquired using a flat-panel digital chest system (XQ/I Revolution, General Electric Medical Systems, Milwaukee, WI) with a posteroanterior projection within 1 week of the CT images. The chest system included a cesium iodide (CsI) scintillator and an amorphous silicon photodiode-transistor array. The detector had an image size of 41×41 cm and a pixel dimension of 0.2×0.2 mm.

Dual-energy radiographs were acquired using a dual-exposure technique with 200 msec between the high- and low-energy exposures. The imaging parameters included a 120 kV image at a speed equivalent to approximately 200, and a 60 kV image at a speed equivalent to approximately 200. In addition to the subtraction techniques, which generated isolated soft-tissue and bone selective images, post-processing algorithms with pixel shifting and noise reduction were used. Routine dual-exposure dual-energy radiographs (DER) consisted of a high kVp standard chest radiograph (SR), a dual-energy subtracted soft-tissue selective image, and a dual-energy subtracted bone selective image. A low kVp radiograph was acquired as baseline data, but was not presented in the routine examinations.

The CT examinations were performed using a multidetector CT (Lightspeed 16, General Electric Medical Systems, Milwaukee, WI). Entire lungs were scanned in single breath-hold mode in the caudocranial direction.

All digital images were forwarded to a picture archiving and communication system (PACS) workstation (Centricity v2.0, General Electric Medical Systems, Milwaukee, WI). All digital images were viewed on a 21 inch monochrome liquid crystal display (LCD) monitor (Totoku, Tokyo, Japan) at a resolution of $2048 \times 2560 \times 8$ bits.

Nodule detection and selection

CT examinations have served as the gold standard in determining the precise size and location of the lesions. Two radiologists; one with experience with dual dual-energy imaging, reviewed the CT images and identified lesions larger than 4 mm and less than 20 mm in diameter by consensus. Calcifications were determined by comparing the lesions with nearby ribs on the tissue window images. The selected lesions were marked on SR.

Forty-three peripheral lung nodules (calcified or non-calcified, mean: 9 mm, range: 4–20 mm, and median: 7.9 mm in diameter) were selected. Twenty-four nodules had calcifications (mean: 10 mm, range 4–20 mm, and median 8 mm in diameter) and 19 (mean: 13 mm,

range: 5-20 mm, and median: 13 mm in diameter) did not. Twenty-eight locations, mimicking the appearance of nodules in SR of the same patients, were used as negative controls. In total, 71 locations were marked on SR.

Image evaluation

All chest radiographs were reviewed by the two radiologists who were unaware of the previous results and the clinical details, including the diagnosis and CT examination results. One of two radiologists had more than 10 years of experience of chest radiology, whereas the other was a trainee.

At first, all chest radiographs were presented as SR alone and 1 week later were presented as DER including SR. All images were viewed on an LCD monitor. A independent review was undertaken by each radiologist. One radiologist, who was an expert at chest imaging, had gained extensive experience with the DER. The other had been trained in the use of DER just prior to this study.

The reviewers were asked two questions about the seventy-one marked lesions in SR. The first question was, "Is this a true nodule?" And, if they responded positively, the next question asked was, "Does this nodule show calcification?" No limit was imposed on the reading time. A continuous rating scale of 0-10 was used to represent the observer's confidence levels.

Statistical analysis

For the statistical analysis, the observer performance in discriminating true nodules and calcified nodules with SR only and with DER were tested using a receiver operating characteristics (ROC) analysis. The decision accuracy was measured using 'areas under the ROC curves' (AUC), as determined by the ROCKIT program (Metz C, University of Chicago, IL).

We calculated the statistical significances of the differences between the AUC values. The adopted confidence interval was 95%, and the significance was accepted at the $p < 0.05$ level. Inter-observer agreement for the discrimination of true nodule and nodule calcification was evaluated using linear weighted κ-statistics. The range of the κ-values can extend from 0 (no agreement) to 1.00 (perfect agreement), and can be interpreted as poor (0), slight (0.01-0.21), fair (0.21-0.40), moderate (0.41-0.60), substantial (0.61-0.80), and almost perfect (0.81-1.00). The statistical analysis was performed using the SPSS package for Windows, release 12.0 (SPSS, Chicago, IL).

Results

Nodule discrimination

The ROC results are shown in Table 1 and Figure 1.

The average AUC values for the discrimination of small nodules were 0.691 for SR alone and 0.744 for

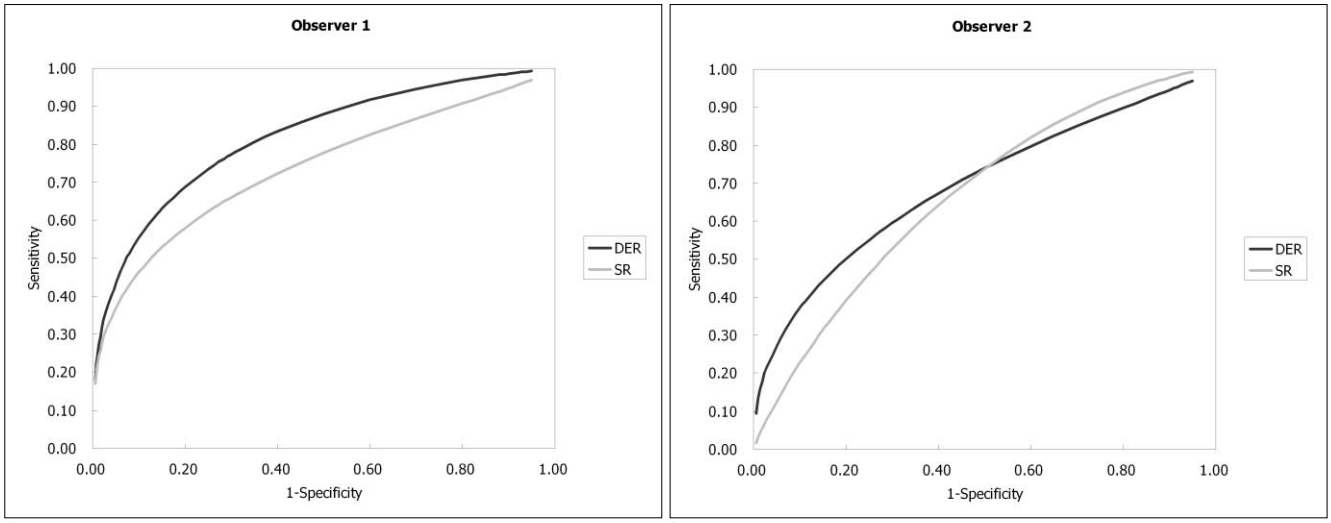

A B

Fig. 1. ROC curves for the detection and discrimination of a true nodule. The ROC curves show no significant difference in the detection of true nodules regardless of the DER images.
A. ROC curve of observer 1.
B. ROC curve of observer 2.
Abbreviations: SR, Standard PA chest radiographs alone; DER, SR in conjunction with dual-exposure dual-energy subtraction images
Observer 1: Experienced, Observer 2: Inexperienced

DER. Moreover, the diagnostic performance in the detection/discrimination of true nodules was higher in DER than SR alone, however the difference was not significant (p = 0.202) (Fig. 2).

Inter-observer agreement between the two observers was moderate for SR alone and DER (κ = 0.391 and 0.529, respectively).

Nodule calcification

The ROC results are presented in Table 2 and Figure 3.

The mean AUC values used for the prediction of nodule calcification were 0.684 for SR alone and 0.949 for DER. The predictability of nodule calcification was significantly greater when comparing DER and SR alone (p < 0.001) (Fig. 4). Moreover, the improvement in the AUC value (ΔAUC) for the DER compared to SR alone,

Table 1. Results of the True Pulmonary Nodule Discrimination

Test Result Variable (s)		AUC	95% Confidence Interval		Interobserver Variation	Mean AUC	Difference
Method	Observer		Lower Bound	Upper Bound			
SR	1	0.713	0.595	0.831	0.513	0.691	p = 0.202
	2	0.668	0.539	0.797			
DER	1	0.795	0.690	0.901	0.080	0.744	
	2	0.692	0.570	0.815			

Abbreviations: SR, Standard Chest Radiographs alone; DER, SR in conjunction with Dual Exposure Dual-Energy Radiographs; AUC, Area Under Curve

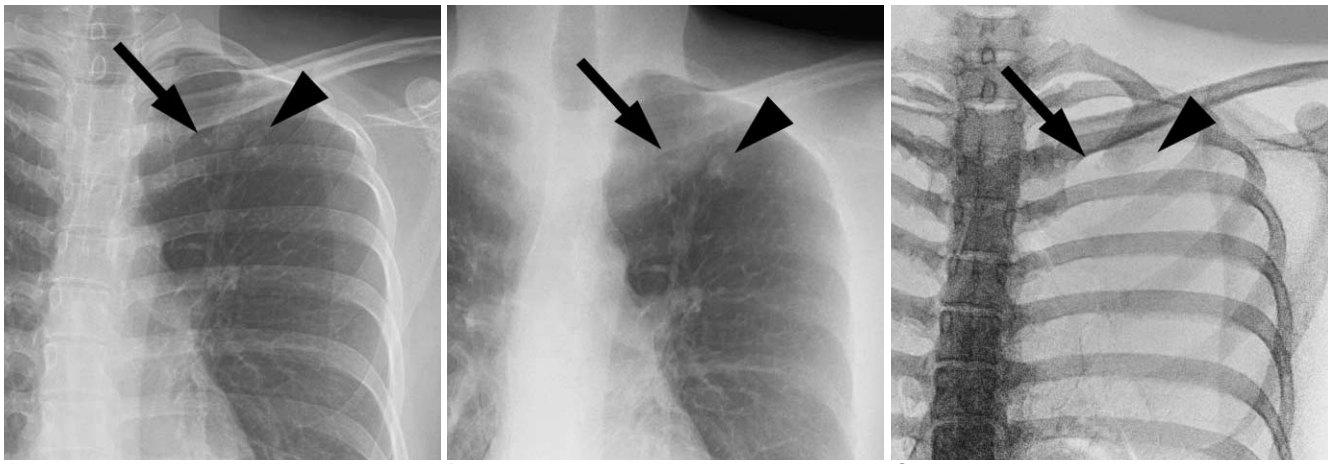

A B C

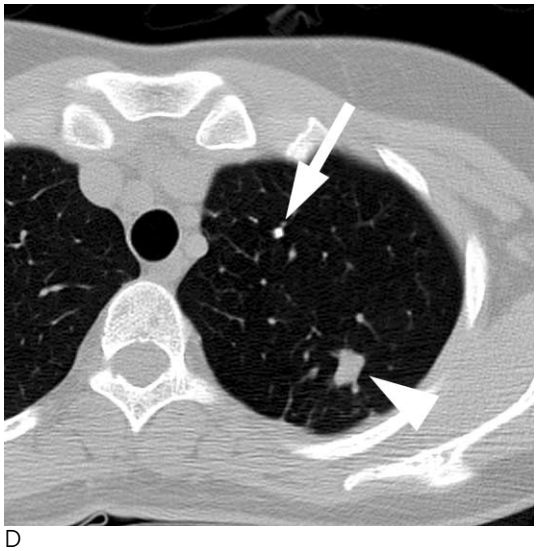

D

Fig. 2. A 65-year-old patient with a chronic cough
A–C. A nodule (arrowhead) obscured by a patient rib on a standard radiograph (A) is more clearly shown with the dual-energy soft-tissue image (B). From the medial aspect, a tiny nodule (arrow) is shown as a calcified nodule in the dual-energy bone-selective image (C).
D. A non-contrast CT scan confirms the diagnosis of a calcified nodule (arrow) and a non-calcified nodule (arrowhead).

was higher for the inexperienced observer (ΔAUC = 0.44) than for the experienced observer (ΔAUC = 0.09).

The inter-observer agreement between the two observers was poor for SR alone but moderate for DER (κ = 0.014 and 0.533, respectively).

Discussion

The detection of pulmonary nodules by conventional chest radiography is of considerable importance, with the presence of calcification within a nodule provides the most reliable evidence of nodule benignity. Rib abnormalities (e.g., bone island or callus formation) and calcified pleural plaques can mimic nodules. To avoid unnecessary further work-up and patient concern, chest radiologists play an important role in nodule detection as well as the prediction of calcification.

In this study, we sought to determine the clinical impact of dual-exposure dual-energy radiography generated by a flat-panel detector used to detection and discriminate true nodules and nodule calcifications.

The results of this study suggest that we could improve true nodule detection by using additional dual energy imaging technique, but not significantly. This result differs from those of previous studies on nodule detection using dual-exposure dual-energy radiography (9, 10). The likely reasons for this discrepancy are:

First, the number of calcified nodules (24/43) was higher than the number of non-calcified nodules (19/43). Since calcified nodules are usually dense, observers detected the nodules more easily. Second, the design of our study was somewhat different from previous studies, which have focused on nodule detection, and thus used unmarked chest radiographs. Our study focused on nodule detection and discrimination; thus, the lesions and pseudo-lesions were already marked on radi-

Table 2. Results of the Prediction for the Pulmonary Nodule Calcification

Test Result Variable(s)		Area	95% Confidence Interval		Interobserver Variation	Mean AUC	Difference
			Lower Bound	Upper Bound			
SR	1	0.853	0.735	0.971	0.000	0.684	$p < 0.001$
	2	0.514	0.336	0.693			
DER	1	0.942	0.866	1.018	0.724	0.949	
	2	0.955	0.892	1.018			

Abbreviations: SR, Standard Chest Radiographs alone; DER, SR in conjunction with Dual Exposure Dual-Energy Radiographs; AUC, Area Under Curve

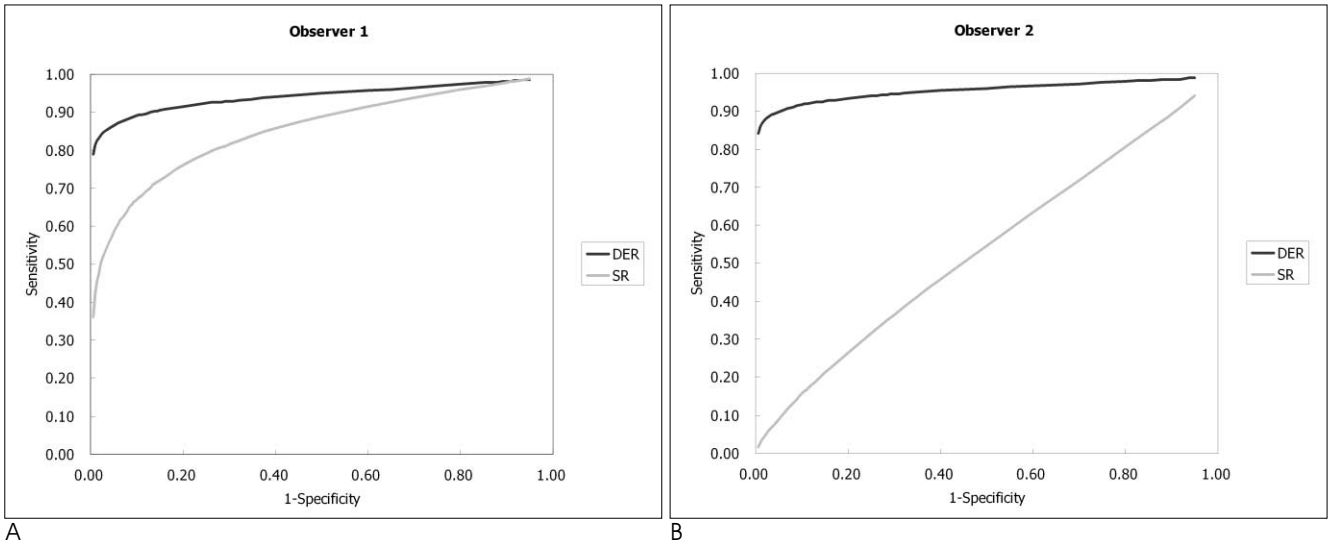

A B

Fig. 3. ROC curves for the prediction of nodule calcifications. ROC curves show improvement in observer confidence in determining calcification with DER images, especially in observer 2.
A. ROC curve of observer 1.
B. ROC curve of observer 2.
Abbreviations: SR, Standard PA chest radiographs alone; DER, SR with dual-energy subtraction images
Observer 1: Experienced, Observer 2: Inexperienced

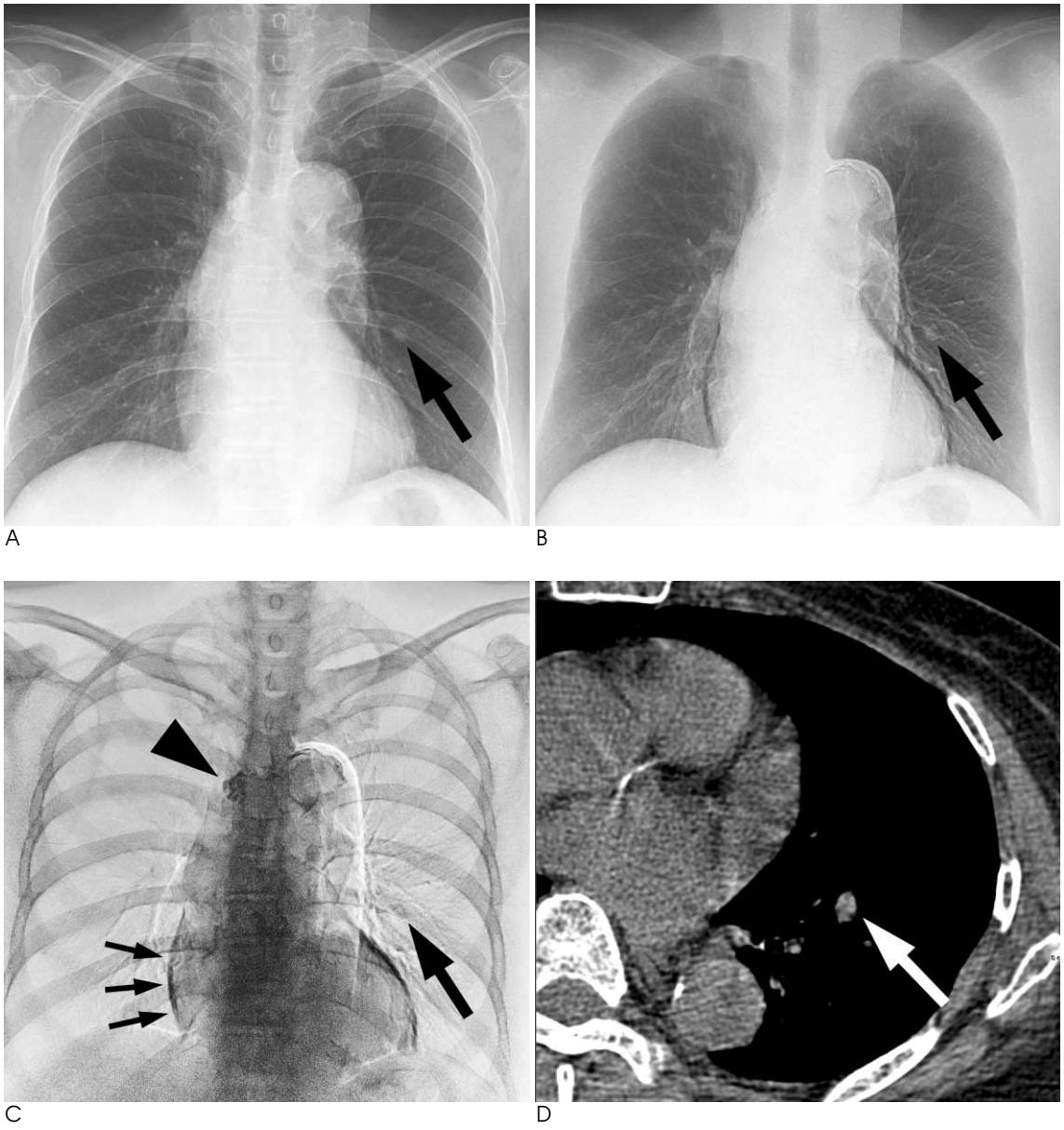

Fig. 4. A 55-year-old patient with no specific symptoms
A, B. A small pulmonary nodule in the left lower lung zone is more evident in the dual-energy soft-tissue image (B) than the standard radiograph (A).
C. Dual-energy bone-selective images show the calcification of the nodule (large arrow). White and black lines (small arrow) show motion artifacts.
D. A non-contrast axial CT scan confirms the calcification of nodule.
E. An additional calcified lesion (arrowhead in C) was identified as a calcified lymph node in left upper paratracheal area.

ographs. Therefore, there was no chance that observers missed a lesion.

In the present study, the predictability of nodule calcification was found to be significantly improved by additional dual-energy imaging. This is supported by the results of previous studies that compared dual-energy images with standard radiographs using flat-panel detector systems (11). Moreover, nodule calcification predictability by the inexperienced radiologist was nearly the same as that of an experienced radiologist when DER+SR were used. Considering that a chest radiography is usually the first screening method used to detect lung cancer, the compensation of experience-dependent differences is important. To the best of our knowledge, no report has evaluated the prediction of nodule calcification utilizing a flat-panel digital chest system and analyzed by the ROC curve.

Two types of dual-exposure dual-energy radiography systems are currently available, (i.e., a single-exposure system and a dual-exposure system). Single-exposure systems used stacked films with a filter between two films to provide a different kVp to the front and back films, whereas the dual exposure system, as employed in the present study, separately exposes the two films at different kVps. In previous studies, single exposure systems using storage phosphor plates or phosphor/photodiode detectors were determined to be useful for detecting pulmonary nodules and chest calcifications (12-14). However, because of inconsistent image quality, workflow inconvenience, the ineffective usage of X-ray, and other reasons, these systems have not been accepted for routine clinical examinations (13-15).

Full-field digital amorphous silicon flat-panel x-ray detector radiography systems based on CsI and amorphous silicon have recently become commercially available. Because its detective quantum efficiency (DQE) is higher than that of computed radiography and film-screen radiography systems, this modality allows radiation dose reduction with less noise (16, 17). A direct comparison of the image quality of the detector-based radiography was found to be superior to that of film-screen and computed radiography (7, 8, 18-22).

In our study, calcifications in the pleura, mediastinum and vascular structures were not evaluated. However, Kuhlman et al. reported that dual-exposure dual-energy subtraction images were also helpful for these types of lesions (23).

In spite of DER aid nodule detection and the prediction of nodule calcification, caution must be exercised prior to diagnosis. First, the 200 msec delay between the two exposures can cause temporal-motion artifacts on the subtracted images (Fig. 4C). Since these artifacts are more easily seen on bone-selective images than soft-tissue selective images, small lesions detected only in bone-selective images may be artifacts or cross-sections of non-subtracted pulmonary vessels. Next, though nodule calcification is the most reliable factor of benignancy, calcified malignant nodules such as an eccentric, punctuate, or partial (<10%) calcifications must not be diagnosed as benign.

We also estimated skin entrance doses using a chest phantom. The phantom entrance dose for standard chest radiographs was 0.31 mGy for the PA shot and 1.41 mGy for the lateral shot. For the dual-exposure dual-energy radiographs, the entrance dose was 0.59 mGy. Thus, the entrance dose was 0.28 mGy greater than the standard chest radiograph alone. The total chest radiography dose, including the PA and lateral images was 16% higher than when dual energy mode was used (1.72 mGy vs. 2.00 mGy). This result is consistent with the studies, which reported an increase of 14% (11). Thus, the radiation exposure dose required for dual-exposure dual-energy radiography, using a flat-panel detector did not significantly increase for the diagnosis rate observed in standard radiography alone with PA and lateral view.

The relatively low sensitivity of dual-energy images for small pulmonary nodules compared to CT images suggests that the dual-energy radiograph is not an appropriate substitute for the CT (24-27). Furthermore, according to our result, nodule detection is not more sensitive than the standard chest radiography. However, dual-exposure dual-energy radiographs can reinforce the standard chest radiograph inexpensively in terms of prediction of nodule calcification. Thus, we propose that chest radiography using dual-exposure dual-energy technique may be suitable for a complementary study when a nodule is detected on a standard chest radiograph.

In conclusion, dual-exposure dual-energy radiography used in conjunction with standard chest radiography provides no additional benefit for the small lung nodule detection and discrimination, but has additional benefit in characterization of calcification in it.

References

1. Berkson J, Good CA, Carr DT, Bruwer AJ. Identification of "posi-

tives" in roentgenographic readings. *Am Rev Respir Dis* 1960;81: 660-665
2. Stitik FP, Tockman MS. Radiographic screening in the early detection of lung cancer. *Radiol Clin North Am* 1978;16:347-366
3. Yerushalmy J. Reliability of chest radiography in the diagnosis of pulmonary lesions. *Am J Surg* 1955;89:231-240
4. Kundel HL. Predictive value and threshold detectability of lung tumors. *Radiology* 1981;139:25-29
5. Webb W. *The solitary pulmonary nodule*. 2nd ed. Baltimore: Williams & Wilkins, 1997:101-118
6. Aufrichtig R. Comparison of low contrast detectability between a digital amorphous silicon and a screen-film based imaging system for thoracic radiography. *Med Phys* 1999;26:1349-1358
7. Spahn M, Strotzer M, Volk M, Bohm S, Geiger B, Hahm G, et al. Digital radiography with a large-area, amorphous-silicon, flat-panel X-ray detector system. *Invest Radiol* 2000;35:260-266
8. Strotzer M, Gmeinwieser JK, Volk M, Frund R, Seitz J, Feuerbach S. Detection of simulated chest lesions with normal and reduced radiation dose: comparison of conventional screen-film radiography and a flat-panel X-ray detector based on amorphous silicon. *Invest Radiol* 1998;33:98-103
9. Ricke J, Fischbach F, Freund T, Teichgraber U, Hanninen EL, Rottgen R, et al. Clinical results of CsI-detector-based dual-exposure dual energy in chest radiography. *Eur Radiol* 2003;13:2577-2582
10. Uemura M, Miyagawa M, Yasuhara Y, Murakami T, Ikura H, Sakamoto K, et al. Clinical evaluation of pulmonary nodules with dual-exposure dual-energy subtraction chest radiography. *Radiat Med* 2005;23:391-397
11. Fischbach F, Freund T, Rottgen R, Engert U, Felix R, Ricke J. Dual-energy chest radiography with a flat-panel digital detector: revealing calcified chest abnormalities. *AJR Am J Roentgenol* 2003; 181:1519-1524
12. Kelcz F, Zink FE, Peppler WW, Kruger DG, Ergun DL, Mistretta CA. Conventional chest radiography vs dual-energy computed radiography in the detection and characterization of pulmonary nodules. *AJR Am J Roentgenol* 1994;162:271-278
13. Niklason LT, Hickey NM, Chakraborty DP, Sabbagh EA, Yester MV, Fraser RG, et al. Simulated pulmonary nodules: detection with dual-energy digital versus conventional radiography. *Radiology* 1986;160:589-593
14. Oestmann JW, Greene R, Rhea JT, Rosenthal H, Koenker RM, Tillotson CL, et al. "Single-exposure" dual energy digital radiography in the detection of pulmonary nodules and calcifications. *Invest Radiol* 1989;24:517-521
15. Kruger RA, Armstrong JD, Sorenson JA, Niklason LT. Dual energy film subtraction technique for detecting calcification in solitary pulmonary nodules. *Radiology* 1981;140:213-219
16. Floyd CE, Jr., Warp RJ, Dobbins JT 3rd, Chotas HG, Baydush AH, Vargas-Voracek R, et al. Imaging characteristics of an amorphous silicon flat-panel detector for digital chest radiography. *Radiology* 2001;218:683-688
17. Garmer M, Hennigs SP, Jager HJ, Schrick F, van de Loo T, Jacobs A, et al. Digital radiography versus conventional radiography in chest imaging: diagnostic performance of a large-area silicon flat-panel detector in a clinical CT-controlled study. *AJR Am J Roentgenol* 2000;174:75-80
18. Fink C, Hallscheidt PJ, Noeldge G, Kampschulte A, Radeleff B, Hosch WP, et al. Clinical comparative study with a large-area amorphous silicon flat-panel detector: image quality and visibility of anatomic structures on chest radiography. *AJR Am J Roentgenol* 2002;178:481-486
19. Hennigs SP, Garmer M, Jaeger HJ, Classen R, Jacobs A, Gissler HM, et al. Digital chest radiography with a large-area flat-panel silicon X-ray detector: clinical comparison with conventional radiography. *Eur Radiol* 2001;11:1688-1696
20. Herrmann A, Bonel H, Stabler A, Kulinna C, Glaser C, Holzknecht N, et al. Chest imaging with flat-panel detector at low and standard doses: comparison with storage phosphor technology in normal patients. *Eur Radiol* 2002;12:385-390
21. Kotter E, Langer M. Digital radiography with large-area flat-panel detectors. *Eur Radiol* 2002;12:2562-2570
22. Okamura T, Tanaka S, Koyama K, Norihumi N, Daikokuya H, Matsuoka T, et al. Clinical evaluation of digital radiography based on a large-area cesium iodide-amorphous silicon flat-panel detector compared with screen-film radiography for skeletal system and abdomen. *Eur Radiol* 2002;12:1741-1747
23. Kuhlman JE, Collins J, Brooks GN, Yandow DR, Broderick LS. Dual-energy subtraction chest radiography: what to look for beyond calcified nodules. *Radiographics* 2006;26:79-92
24. Diederich S, Lenzen H, Windmann R, Puskas Z, Yelbuz TM, Henneken S, et al. Pulmonary nodules: experimental and clinical studies at low-dose CT. *Radiology* 1999;213:289-298
25. Naidich DP, Marshall CH, Gribbin C, Arams RS, McCauley DI. Low-dose CT of the lungs: preliminary observations. *Radiology* 1990;175:729-731
26. Rusinek H, Naidich DP, McGuinness G, Leitman BS, McCauley DI, Krinsky GA, et al. Pulmonary nodule detection: low-dose versus conventional CT. *Radiology* 1998;209:243-249
27. Takahashi M, Maguire WM, Ashtari M, Khan A, Papp Z, Alberico R, et al. Low-dose spiral computed tomography of the thorax: comparison with the standard-dose technique. *Invest Radiol* 1998;33: 68-73

J Korean Radiol Soc 2008 ; 59 : 385-393

대한영상의학회지 2008 ; 59 : 385-393

이중노출 이중에너지 방사선촬영술과 단순흉부방사선촬영술의 소폐결절 진단에 대한 비교[1]

[1]성균관대학교 의과대학 삼성서울병원 영상의학과
[2]강원대학교 의과대학 영상의학과

황혜선 · 정명진 · 김성목 · 이지원[2] · 한 헌[2]

목적: 이중에너지 방사선촬영술(dual energy radiography, DER)의, 폐결절의 식별과 이 결절들의 석회화 유무를 판별하는 데 대한 가치를 평가하고자 하였다.

대상과 방법: DER과 흉부 전산화단층촬영(Computed tomography, CT)을 같이 시행 받은 29명의 환자를 대상으로, 43개의 변연부 폐결절을 선택하였다. 이 중 24개의 결절은 CT상에서 석회화를 포함하고 있었고 19개는 그렇지 않았다. 단순흉부촬영(standard chest radiography, SR)에서 CT로 확인된 28개의 가성 결절을 골랐다. 두 명의 영상의학과 의사가 총 71개의 표시된 위치를 SR과 DER에서 각각 관찰하여, 결절의 존재 여부와 결절의 석회화 유무를 판단하였다. 각 관찰자는 0-10의 순차적 등급순위를 적용하여 판단의 신뢰도를 정량화하였으며 이를 ROC 분석하였다. SR단독과 DER조합의 각각에서 ROC 분석의 곡선하면적(AUC)을 계산하여 비교하였다.

결과: 폐결절의 판별능은 SR 단독보다 DER에서 높았으나, 그 차이는 통계적으로 유의하지 않았다(p = .202). 관찰자 간 일치도는 SR과 DER에서 모두 보통 수준이었다. 결절 내 석회화 유무의 판별능은 SR 단독보다 DER에서 유의하게 높았다(p 〈 .001). 관찰자간 일치도는 SR에서 미약하였으나 DER에서는 보통 수준이었다.

결론: SR에 추가 적용되는 DER은 폐결절의 판별에 추가적인 이익은 없으나 폐결절의 석회화 감별에는 도움이 된다.